

Improving the bus flow in a Bus Rapid Transit system: an approach based on cellular automata simulations

M. A. Uribe-Laverde*, W. F. Oquendo-Patiño

*Grupo de Investigación en Física y Matemáticas Aplicadas, Faculty of Engineering,
Universidad de La Sabana, CO-250001 Chía, Colombia*

Abstract

We studied the bus flow in a Bus Rapid Transit (BRT) system using a novel approach based on a cellular automata (CA) that properly accounts for bus interactions. The model quantitatively reproduces the bus queuing behaviour for both fixed and random dwell times, with one bus service. For more bus services, our results show that the bus flow strongly depends not only on how the buses are distributed among the services, but also on how the bus stops are physically arranged at the stations. The latter dependence has hitherto not been considered in common BRT optimization methods. By using a genetic algorithm, we could find the bus distribution that maximizes the bus flow for a given stops arrangement at the stations, and explore its evolution with the bus density. Our results suggest a set of guidelines which could be applied on working BRT systems to improve the bus flow.

Keywords: Bus Rapid Transit systems, bus flow optimization, microsimulation, cellular automata, simheuristics

Declaration of interests: None

1. Introduction

A Bus Rapid Transit (BRT) system consists of a dedicated corridor, typically with a length of several kilometers, where buses are able to move between stops without the interference of private vehicles. Additional features of BRT systems often include platform-level boarding, off-board fare collection, busway and station alignment to the center of the street, and the implementation of limited-stop services that skip some stations and thus have larger average speeds [1, 2]. As a result, BRT systems offer a high-capacity and cost-effective public transportation alternative to the more expensive railway-based systems. Although BRT-type systems were proposed as early as the 1930s, it is only in

*Corresponding author: miguel.uribe1@unisabana.edu.co

recent decades that these systems have been increasingly implemented in several mayor cities in the world like Sao Paulo, Rio de Janeiro, Bogotá, Istambul, Guangzhou or Lima [3].

Nevertheless, to maximize the transport capacity of a BRT system careful planning should be performed. In particular, a set of limited-stop services must be designed, and their frequencies optimized, to find a balance between the advantages of lower traveling times and the disadvantages of larger waiting times at the stations, more transfers and heavily loaded buses. This is an extremely difficult problem whose proper solution becomes relevant for systems implemented in densely populated areas like Bogotá, Colombia or Rio de Janeiro, Brasil, where the peak load can be as large as 48000 and 65400 passengers per hour per direction, respectively [3]. Research on this field is scarce and methods to solve the limited-stop service design and frequency optimization problem have become available only in the last ten years. Most of these methods incorporate an objective function that takes into account both, the cost in time for the users and the operation costs. This function, which is non-linear, is subsequently minimized subjected to fleet availability constraints [4, 5, 6, 7, 8, 9].

An important limitation of these methods lies in the difficulty to incorporate the delays caused by the interaction between buses into the objective functions. In practice, the interaction between buses is reduced by introducing a passing lane at stations to allow for stop-skipping services to pass the stopping buses. In addition, stations consist of several docking bays where different bus services stop without interfering each other. However, it has been established that the bottleneck of BRT systems is at the busiest docking bays, where queues of buses appear affecting the bus flow of the entire system [10, 11, 1]. In heavily loaded systems, as the ones already mentioned in Bogotá or Rio de Janeiro, queues at the busiest stations are simply unavoidable and affect the overall performance of the system. Mathematical models have been proposed to take into account the delays due to bus queues at stations. However, these models have been used mainly to simulate and characterize the bus behaviour at stations [12, 11], they have not yet been implemented into the objective function of an optimization scheme. To the best of our knowledge, the queueing effect has not been properly taken into account in the published research on the BRT route design and frequency optimization problem. It is thus expected that these methods would fail to provide optimal solutions in heavily loaded systems where queues at the busiest stations limit the bus flow.

In our group, we are currently working on a different approach to this problem based on simulations performed using a cellular automata (CA) algorithm. If the simulation model is accurate, this approach could effectively account for the interaction between buses and could also successfully integrate all the stochastic parameters that are inherent to the BRT system operation. The use of CA models to simulate traffic was first proposed in 1993 by Nagel and Schreckenberg [13]. With time, more elements have been introduced into the model to

simulate complex driving behavior and allow for multiple-lane highways [14, 15]. Applications of the CA models in traffic research are still common in the scientific literature [16, 17, 18, 19]. In the field of simulation of BRT systems, CA models have already been implemented to study passenger accumulation at bus stations [20], study passenger waiting times in single-lane and single-service BRT systems [21], and to model bus queues and station capacity using commercially available microsimulation packages [22]

As a first step towards a CA based approach to the optimization of a BRT system, in this work, not yet considering passengers, we focus on the study of the bus flow and its dependence on the bus density, the bus distribution among the bus services, and the arrangement of the stops at the stations. Our results show that the CA model properly reproduces the bus interactions leading to operation delays. Additionally, combining the CA simulations and a genetic algorithm, we use the results of the simulations to find the bus distribution among the bus services that maximizes the bus flow. Interestingly, we find that the bus flow in the system strongly depends on how the docking bays are assigned to each bus service at the stations. An effect that, to the best of our knowledge, has not yet been considered when proposing solutions to the route design and frequency optimization problem in BRT systems. Despite not considering the influence of passengers in our study, our results allow us to provide a set of guidelines, which might readily contribute to enhance the transport capacity in real working BRT systems.

The paper is organized as follows: in Section 2, the system layout, the CA model and the simulation process are described; in Section 3 the model is validated by contrasting the simulation results when only one bus service is implemented in the BRT system against known bus behaviour; in Section 4 the results when more bus services are implemented are presented and a bus flow optimization scheme is applied, our findings on the dependence of the bus flow on the docking bay arrangement are discussed; in Section 5 our conclusions and a set of guidelines to enhance the bus flow in BRT systems are provided.

2. Model

In this section we describe the BRT system layout and the limited-stop services that were implemented. We also introduce the CA model that we used to simulate the bus behaviour and to study the bus flow in the BRT system. Finally, we provide details about the simulation process.

2.1. The system layout

We have created a periodic bus corridor with a total of 45 stations. Space is discretized with cells of constant length $\delta x = 3$ m, and the possible state of each cell is either occupied by a bus or empty. Time is also discrete, and each time-step lasts $\delta t = 1$ s. The stations are uniformly distributed along

the corridor with a spatial periodicity of 235 cells=705 m. The structure of the stations is shown in Figure 1 and is inspired by the stations in Transmilenio, the BRT system in Bogotá, Colombia. Each station consists of three substations separated by pedestrian corridors. In each substation, there is a docking bay where a bus can stop to allow passengers for boarding or alighting. The length of a substation and their spatial periodicity are set to 15 cells=45 m and 30 cells=90 m, respectively. As also shown in Figure 1, in the region between stations the corridor consists of a single main-lane. However, to allow buses to stop without disrupting the stop-skipping services, in the vicinity of the stations a stopping-lane is introduced. This lane configuration is also inspired by Transmilenio. It should be noted that any other station or lane arrangements, as well as other elements such as traffic lights, could easily be introduced into the model.

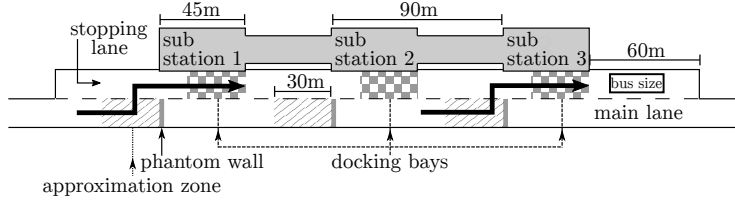


Figure 1: Schematic diagram of the stations in the simulated BRT system. Each station consists of three substations, the buses stop at the docking bays, which are located at the end of each substation, in the downstream direction, and are marked by a checker pattern. Buses can only change from the main to the stopping lane in the stripe-patterned approximation zones. The arrows depict the expected approximation path of a bus. For reference, the bus size is also shown on the right side of the diagram.

As shown in Figure 2, four different bus services have been created to study and optimize the bus flow of the BRT system. Service E1 is a regular service that stops at every station. Services E3, E5 and E9 are limited-stop services that stop every three, five, and nine stations, respectively. The middle station of the system has been chosen as the main hub, this is the only station where all four services stop.

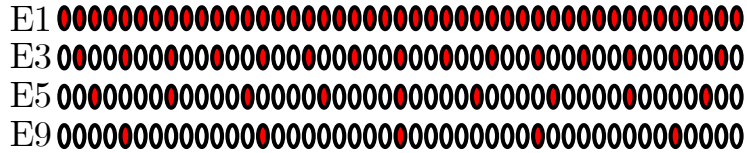


Figure 2: Stop distribution of the bus services in the BRT system. The 45 ellipses represent stations, a filled station represents a stop. Service E1 is a regular service that stops at every station. Services E3, E5 and E9 are limited-stop services, which skip most of the stations in the system.

Since we are interested in the dependence of the bus flow on the bus density,

only one direction of movement has been considered and periodic boundary conditions have been implemented at the ends of the corridor.

2.2. The cellular automata model

The rules controlling the forward motion of the buses are the usual for the Nagel and Schreckenberg (NaSch) model and can be summarized in three steps [13, 23]:

- Acceleration and breaking:

$$v_i(t) = \min\{v_i(t-1) + 1, g_i(t-1), v_{\max}\}. \quad (1a)$$

- Randomization:

$$\text{If } \xi_i(t) < p, \text{ then } v_i(t) = \max\{0, v_i(t) - 1\}. \quad (1b)$$

- Movement:

$$x_i(t) = x_i(t-1) + v_i(t). \quad (1c)$$

In rule (1a), $v_i(t)$ corresponds to the velocity of bus i in time-step t , $g_i(t)$ corresponds to the free space in the forward direction for bus i in time-step t , and $v_{\max} = 7 \text{ cells/s} = 75.6 \text{ km/h}$ corresponds to the maximal velocity of the buses. This rule implies that all buses tend to accelerate with a constant rate of 1 cell/s^2 unless they either find an obstacle with which they are about to collide (in this case they brake to avoid collision), or they reach the maximal velocity (in this case they no longer accelerate).

Rule (1b) introduces a stochastic element to the model that is necessary to reproduce realistic behaviour [14]. At each time-step, and for every bus, a random number $0 \leq \xi_i(t) < 1$ is generated. If this number is smaller than a random breaking probability, $p = 0.25$, the bus decreases its velocity by one. As a consequence of rule (1b), the cruise speed of the buses in the NaSch model is reduced to [14]

$$v_{\text{ns}} = v_{\max} - p \text{ cells/s} = 6.75 \text{ cells/s} = 72.9 \text{ km/h}. \quad (2)$$

Finally, in rule (1c) the bus advances by a number of cells $v_i(t)$ and it is now located at cell $x_i(t)$. It should be mentioned that a single bus spans over 10 cells to reproduce a realistic bus length of 30 m. In this way, $x_i(t)$ corresponds to the cell where the head of the bus is located.

The calculation of the quantity g_i for a given bus depends on whether the bus is on the main lane or in the stopping lane. In the former case, g_i is calculated as the minimum between the distance to the bus in front and the distance to the next phantom wall. The phantom walls are introduced to force buses to change to the stopping lane when approaching a docking bay where they are

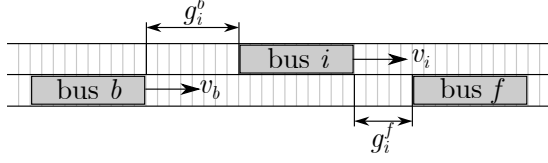


Figure 3: Definition of gaps g_i^b and g_i^f , and the speeds v_i and v_b . These quantities are taken into account when bus i attempts to change lane according to the rule defined by Equation 3.

going to stop. As shown in Figure 1, a docking bay's phantom wall is located at an upstream distance of 15 cells=45 m from the platform position. On the other hand, if the bus is in the stopping lane, g_i is calculated as the minimum among the distance to the bus in front, if any; the distance to the end of the lane; and the distance to the docking bay in case it has not yet reached it. As shown in Figure 1, the end of the stopping lane is located 20 cells=60 m downstream from the docking bay position at substation 3.

The lateral motion of the buses is only allowed in the region where two lanes are present. There are two criteria to be fulfilled when changing lanes:

- Safety:

$$v_b(t) < g_i^b \text{ and } v_i(t) < g_i^f, \quad (3)$$

where bus b is the bus behind bus i , in the opposite lane; g_i^b is the gap between bus i and bus b ; and g_i^f is the gap between bus i and the bus in front, in the opposite lane. A schematic definition of all gaps is shown in Figure 3.

- Willingness:

A bus in the main lane is willing to change lanes when it is located in the approximation zone of its next stop. Depicted as the stripe-patterned regions in Figure 1, approximation zones span over 15 cells=45 m and end at the location of the phantom walls. A bus in the stopping lane is willing to change back to the main lane when it has departed from its docking bay and finds an obstacle ahead. This obstacle may be a bus at a different docking bay or the end of the stopping lane.

In the case where jammed buses are found in both the main and the stopping lanes, an additional rule has been introduced to give priority to the buses in the stopping lane that have already stopped at their docking bay.

When a bus reaches a docking bay, it remains stopped for a dwell time of τ time-steps. In our study we have considered two cases: in the first case, the dwell time, τ , is assumed constant and equal for all buses; in the second case, the dwell time for each bus and at each stop is randomly chosen using a Poisson distribution whose mean value is the same for all buses. The latter is a more realistic case: the passengers can be considered as independent events and accumulate with time at the stations following a Poisson distribution, and the dwell

time has been found to be proportional to the number of passengers boarding and alighting at the stations [1]. This is, of course, an over simplification of the passenger accumulation problem which should be properly addressed when passengers and transfer matrices are included into the model.

2.3. The simulation process

Finally, we describe how the simulations are performed. To run a single simulation, the number of buses assigned to each service (N_{E1} , N_{E3} , N_{E5} , N_{E9}) is given as an input. The total number of buses, $N = \sum_l N_l$, is initially uniformly distributed over the entire corridor and the services are assigned randomly according to the required distribution. To keep the number of buses, hence the density, constant, we introduce periodic boundary conditions at the end and at the beginning of the corridor. The system is set to initially evolve for 5000 time-steps, and subsequently the average speed of the entire system is averaged over time intervals of 2000 time-steps. The simulation stops when the relative standard deviation of the averaged system speed calculated over the last 10 time intervals falls below 1%, at this point the system is considered to be in a steady state, independent of the initial conditions. The average speed for each bus service is obtained by averaging the speed over all buses assigned to it. In this research, we are interested in the optimization of the bus flow, which is a quantity directly related with the system capacity to effectively transport passengers. The flow per bus service and the overall flow of the system, respectively, are calculated as follows:

$$q_l = \rho_l \bar{v}_l = \frac{1}{L} \sum_{i=0}^{N_l} \bar{v}_i = \frac{1}{h_l}, \quad (4a)$$

$$q = \rho \bar{v} = \frac{1}{L} \sum_{i=0}^N \bar{v}_i = \sum_{\text{services}} q_l. \quad (4b)$$

In the last two equations, $L = 10575 \text{ cells} = 31725 \text{ m}$ is the total length of the system, \bar{v}_i corresponds to the average speed of bus i , \bar{v} is the speed averaged over all buses, N is the number of buses, q is the bus flow, h is the average headway (time separation between buses), and ρ is the system's bus density; the subindex l indicates that a quantity is related to a specific bus service.

3. Model validation

To test the capacity of our CA model to effectively reproduce realistic behaviour in BRT systems, we investigated the fundamental diagram for each bus service. In the fundamental diagram, the bus flow dependence on the bus density is studied. In consequence, we assigned all buses in the system to the same bus service and studied the overall bus flow as a function of the bus density. Two cases have been considered: in the first one the dwell time is fixed to $\tau = 15 \text{ s}$; in the second case the dwell time at each stop is randomly chosen using a Poisson distribution with mean $\tau = 15 \text{ s}$.

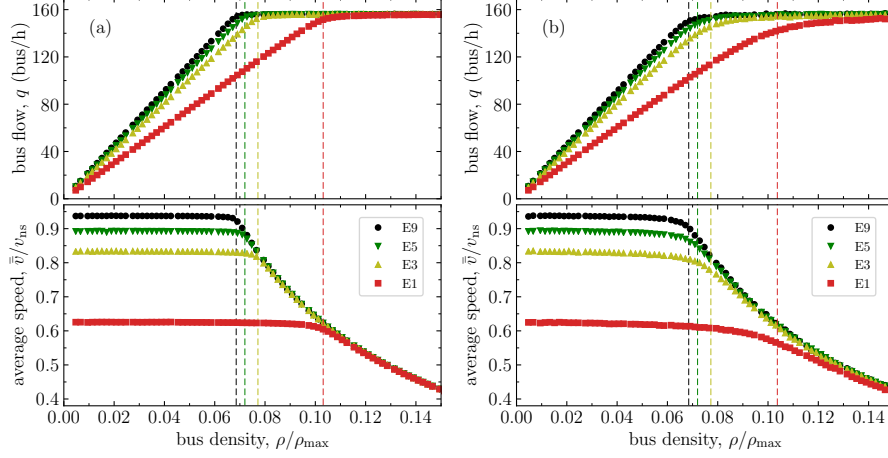


Figure 4: (color online) Bus flow (upper panels) and average bus speed (lower panels) as a function of the bus density for different bus services when only one bus service is in operation. In panel (a), for all buses and at every stop the dwell time is set to $\tau = 15$ s. In panel (b), the dwell time at every stop is randomly generated using a Poisson distribution with mean $\tau = 15$ s. The vertical dashed lines are located at the critical density for each bus service computed using Equation (9). The standard deviations are in all cases smaller than the markers.

Figures 4(a) and 4(b) show the results obtained when the dwell time is fixed, and randomly chosen, respectively. The upper and lower panels in the figures exhibit the bus flow and average bus speed, respectively. The average speed is normalized to the cruise speed in the NaSch model, v_{ns} , and the bus density is normalized to its maximal value, $\rho_{\max} = 1/10 \text{ cells}^{-1} = 1/30 \text{ m}^{-1}$, which is obtained when the entire corridor is occupied by a continuous line of buses. At low densities, the advantages of stop-skipping services are evident: as the frequency of the stops decreases, the buses move faster and fewer buses are thus needed to reach a certain bus flow.

In the case where the dwell time is fixed, Figure 4(a), the fundamental diagram for each bus service can be clearly split into two regions: the so-called uncongested and congested regimes. In the uncongested regime, found at low densities, the buses are naturally spaced by the uniform dwell time at the stations. Therefore, interactions between buses are avoided, the average bus speed is independent of the density, and the bus flow increases linearly with the number of buses.

At a certain critical density, which depends on the frequency of the stops, there is a sharp crossover to the congested regime. At this point the minimum headway has been reached and buses start to queue at the stations. As shown in

Figure 4(a), a further inclusion of buses would not result in an enhancement of the bus flow but in a reduction in the average speed of the system. In the congested regime the system has achieved its maximal transport capacity.

To validate the simulation results, we proceed to contrast them against a quantitative study of the system. As described in the Supplementary Material, Ref. [24], the average speed for bus service l in the uncongested regime can be written as

$$\bar{v}_l^{\text{uc}} = v_{\text{ns}} \frac{1}{1 + \frac{\tau_{\text{eff}}^{\text{uc}} v_{\text{ns}}}{d_l}}, \quad (5)$$

where v_{ns} is the cruise speed in the NaSch model given by equation (2), d_l is the spatial periodicity of the stops for service l , and $\tau_{\text{eff}}^{\text{uc}}$ is the effective dwell time in the uncongested regime. The latter is expected to be the same for all bus services and larger than the nominal dwell time, $\tau = 15$ s, as it includes the time it takes for a bus to break and accelerate back to cruise speed.

Using the average speed in the uncongested regime, shown in the lower panel of Figure 4(a), and equation (5), we have determined the effective dwell time $\tau_{\text{eff}}^{\text{uc}}$. As detailed in the Supplementary Material, Ref. [24], the effective dwell time is found to be service independent. Its value, averaged over all the bus services, is $\tau_{\text{eff}}^{\text{uc}} = 21.1(1)$ s. The extra 6.1 s with respect to the nominal dwell time are a direct consequence of the evolution rules in our CA model, to adjust this parameter to measured values in a real system, the p parameter in our CA model could be tuned, or the CA model itself could be further improved [14].

In the congested regime, queues form at the stations and the bus headway is given by $\tau_{\text{eff}}^{\text{c}}$, the effective dwell time in the congested regime. The bus flow in this regime is therefore given by the departure rate at the stations

$$q_l = 1/\tau_{\text{eff}}^{\text{c}}, \quad (6)$$

a quantity that depends neither on the bus density nor on the bus service. Averaging the bus flow over all services in the congested regime, we obtain the maximal bus flow for a single docking bay:

$$q_{\text{db}} = 156.0(4) \text{ buses/hour}. \quad (7)$$

It corresponds to an effective dwell time in the congested regime of $\tau_{\text{eff}}^{\text{c}} = 23.072(3)$ s, which is about 2 s larger than in the uncongested regime due to the interaction between buses in the queues. From this point forward in this paper, the maximal bus flow for a single docking bay, q_{db} , will be used as the reference unit of bus flow.

According to equation (4a), the average speed of a bus service in the congested regime is given by

$$\bar{v}_l^{\text{c}} = \frac{1}{\rho \tau_{\text{eff}}^{\text{c}}}. \quad (8)$$

Hence, it is inversely proportional to the density and it does not depend on the periodicity of the stops. Both features are observed in the data shown in the lower panel of Figure 4(a).

The critical density for each bus service can be defined as the density at which the average speed in the uncongested and congested regimes are equal. Combining Equations (5) and (8), it can be written as

$$\rho_l^{\text{cr}} = \frac{1}{\bar{v}_l^{\text{uc}} \tau_{\text{eff}}^{\text{c}}} = \frac{1 + \frac{\tau_{\text{eff}}^{\text{uc}} v_{\text{ns}}}{d_l}}{v_{\text{ns}} \tau_{\text{eff}}^{\text{c}}}. \quad (9)$$

Ignoring the slight difference between $\tau_{\text{eff}}^{\text{c}}$ and $\tau_{\text{eff}}^{\text{uc}}$, the critical density in Equation (9) can be interpreted as the density at which the average distance between buses, $1/\rho_l$, matches the average distance a bus travels in the uncongested regime while a bus makes a stop, $\bar{v}_l^{\text{uc}} \tau_{\text{eff}}^{\text{c}}$. This is the density at which buses start to queue. The vertical dashed lines in Figure 4 correspond to the calculated critical densities using Equation (9). The good agreement between the position of the lines and the crossover from the uncongested to the congested regime testifies to the robustness of the results obtained using our CA model. It is also worth mentioning that no sizeable changes in the fundamental diagrams are observed when the system is doubled in size [24]. Therefore, our simulations are not affected by size effects.

Figure 4(b) exhibits the results obtained in the case where the dwell time is randomly chosen at each stop using a Poisson distribution with mean $\tau = 15$ s. This is a more realistic case, the dwell time of a bus depends on the number of passengers boarding or alighting at a given station, both of which can be modelled using Poisson distributions.

As shown in Figure 4(b), when a random dwell time is introduced the fundamental diagrams are similar to the ones obtained for a fixed dwell time, but appear smoothed. Since the dwell time is not uniform, buses could interact even at low densities. Therefore, the average bus speed for all services decreases slowly but continuously as the density increases. Bus queues can appear at all densities and it is not possible to talk about uncongested and congested regimes.

According to the BRT Planning Guide, Ref. [1], the average length of the bus queues, expressed in number of buses, at a docking bay when a random dwell time is introduced in the system is given by:

$$Q = \frac{1}{2} (I_{\text{arr}} + I_{\text{dep}}) \frac{x^2}{(1 - x)}, \quad (10)$$

where $I_{\text{arr/dep}}$ is the irregularity of arrivals/departures at the docking bay, defined as the ratio between the variance and the squared mean of the arrival/departure times, and $x = q\tau_{\text{eff}}^{\text{c}} = q/q_{\text{db}}$ is the docking bay saturation level, defined as the probability of finding a docking bay occupied by a bus. Since

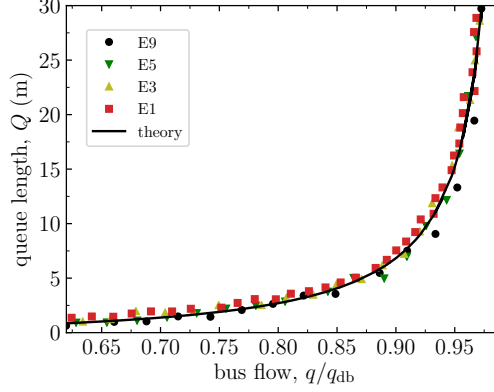


Figure 5: (color online) Average queue length at the docking bays as a function of the bus flow for the bus services E1, E3, E5 and E9 when only one bus service is in operation. The continuous line represents the expected behaviour according to equation (12).

in our BRT system all the stations are expected to behave in the same way, the irregularity of arrivals and departures are the same. The irregularity of departures is directly related to the random nature of the dwell time and can be calculated as:

$$I_{\text{dep}} = \frac{\tau}{\tau_{\text{eff}}^c}, \quad (11)$$

where we have taken into account that the variance in the departures is given by the variance in the nominal dwell time: $\sigma_\tau^2 = \tau$, and that the average dwell time corresponds to the effective dwell time in the congested regime τ_{eff}^c . The average queue length in equation (10) can thus be written, in terms of the bus flow, as:

$$Q = \tau \frac{q^2}{(1 - q\tau_{\text{eff}}^c)}. \quad (12)$$

In the last equation the distance between stops does not appear explicitly, the average queue length at a docking bay only depends on the bus flow and on the average time a bus is stopped.

Based on the data shown in Figure 4(b), we have plotted the queue length as a function of the bus flow for all bus services. The queue length has been determined from the average speed and assuming that the bus average speed in the queues is $10 \text{ cells}/\tau_{\text{eff}}^c$, where 10 cells is the bus length [24]. The results are shown in Figure 5, where the theoretical relationship in equation (12) has also been plotted. In good agreement with theory, data for all services collapse into one single curve and show that when the bus flow is larger than $0.9q_{\text{db}} \simeq 140 \text{ buses/hour}$, queues at the stations start to increase significantly in size. Remarkably, the coincidence between the simulation results and the prediction of the queueing theory is excellent. These results testify to the capability of our CA model to reproduce realistic queueing behaviour at the docking

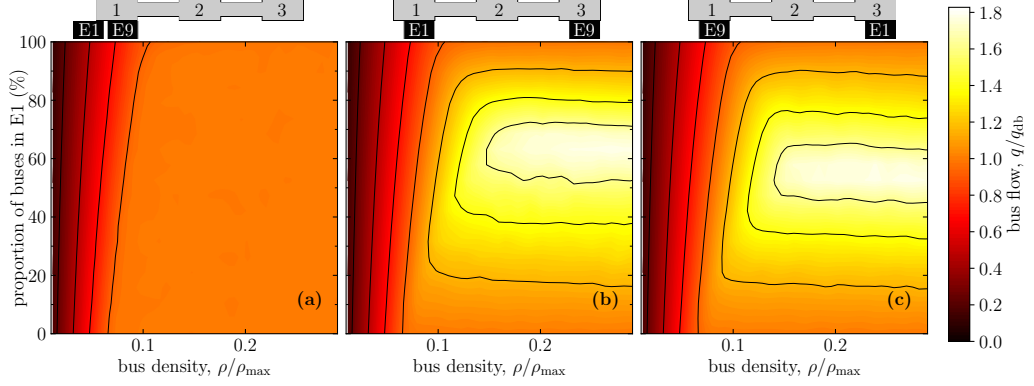


Figure 6: (color online) Bus flow of the BRT system when services E1 and E9 are used. The maps show the dependence of the bus flow on the bus density and the proportion of buses assigned to service E1 for: (a) assignment $\{E1-E9; ;\}$, (b) assignment $\{E1; ;E9\}$, and (c) assignment $\{E9; ;E1\}$. The dwell time is randomly chosen at every stop using a Poisson distribution with mean $\tau = 15$ s. The solid lines correspond to contour lines.

bays when a random nominal dwell time is introduced.

4. Simulation results and flow optimization

In order to improve the bus flow, hence the transport capacity of the system, most BRT systems introduce a combination of bus services. As a consequence, several new degrees of freedom appear. Besides the bus density and dwell time, the bus flow depends on the number of buses assigned to each bus service and on the way the docking bays at the stations are assigned to the bus services. In this section, we use our CA model to study all these dependences when two or more services are in operation. We also propose a bus flow optimization algorithm and study the evolution with the bus density of the optimal bus distribution among the available services.

4.1. Implementation of two bus services and bus flow maps

We start our analysis with the simplest case where two services, namely E1 and E9, are in operation. To trace the dependence of the average bus flow on the new degrees of freedom in the system, we have mapped it considering three variables: the overall bus density, the proportion of buses assigned to each service, and the docking bay assignment at the stations. In all the simulations, the dwell time for every bus stop is randomly chosen using a Poisson distribution with mean value $\tau = 15$ s.

As shown in the upper diagrams in Figure 6, three different substation assignments have been studied. Figure 6(a) shows the obtained bus flow map for assignment $\{E1-E9; ;\}$, where both services stop at substation 1. Figure 6(b) depicts the bus flow map for assignment $\{E1; ;E9\}$, where service E1 stops at

substation 1 and service E9 stops at substation 3. Finally, the results for assignment $\{E9; E1\}$, where services E9 and E1 stop at substations 1 and 3, respectively, are shown in Figure 6(c). The notation for the substation assignments introduced in this paragraph will be used through the rest of the document.

At low bus densities, the behaviour observed in the three maps in Figure 6 is identical: the bus flow increases with the number of buses and increases faster with the bus density the fewer(more) buses are assigned to service E1(E9).

Striking differences appear at higher densities, above the saturation densities of the individual bus services. For assignment $\{E1-E9; ;\}$, shown in Figure 6(a), the flow is observed to be independent of either the bus density or the bus distribution among the services. The value of the maximal bus flow is identical to the bus flow obtained when only one service is implemented $q_{db} = 1/\tau_{eff}^c = 156$ buses/hour. This effect can be understood in terms of queuing of all buses at the stations where the two services overlap. The transport capacity of the system is not enhanced when two lines are assigned to the same docking bay.

On the other hand, when the services E1 and E9 stop at different substations, as shown in Figures 6(b) and 6(c), the overall behaviour of the system is improved. First, the critical density of the system shifts to larger values, which implies that the system can accommodate more buses before the appearance of queues at the docking bays. Second, as more buses are allowed to move in the system without interference a larger bus flow is also observed. Notably, there is an optimal distribution of buses for which a maximal bus flow of about $1.79 q_{db}=280$ buses/hour is obtained. The system capacity is thus enhanced by 80 % with respect to the case where only one docking bay is used. Moreover, the optimal distribution depends on the assignment of the stops at the stations. For assignment $\{E1; ;E9\}$, shown in Figure 6(b), the maximal bus flow is obtained when 63% of buses are assigned to service E1. In the inverse configuration, shown in Figure 6(c), the maximal flow is obtained when 55% of buses are assigned to service E1. We remark that the dependence of the optimal configuration on the substation assignment is a direct consequence of the interaction of buses in the vicinity of the stations, is is thus an effect that cannot be predicted by optimizing methods where the interaction between buses is neglected.

The bus flow of the individual services in the optimal configuration in Figures 6(b) and 6(c) is similar and depends on the substation assigned to the bus service. In both cases, at large densities the bus flow for the service stopping at substation 1 is close to q_{db} , which indicates a large docking bay saturation and the presence of queues. On the other hand, for both substation assignments the bus flow for the bus service stopping at substation 3 corresponds to $0.80 q_{db}=126$ buses/hour, even at high densities, which indicates that substation 3 has maximal saturations of 80 %. Therefore, in the optimal configuration significant queues do not appear at substation 3 and appear only at substation 1. As will be discussed later, this feature is always found in the optimal configu-

rations at high densities, regardless the number of bus services in operation.

As shown in Figure S2 of Ref. [24], a similar behaviour is observed when services E9 and E5 are combined. The flow is not improved when both services stop at the same substation. And in the cases where the services stop at different positions the bus flow is maximized at an optimal bus distribution that depends on the assignment of the docking bays at the stations. Since services E9 and E5 only overlap in one of the 45 stations in the system, we conclude that the performance of the entire system can be affected by the bus interactions at one single station.

4.2. Multiple bus services and flow optimization

As more bus services are in operation in the BRT system, the bus flow mapping procedure applied above becomes more time consuming and, in consequence, of no practical use. To obtain the distribution of buses among the available services that optimizes the bus flow, a multivariate optimization algorithm needs to be implemented. Given the integer nature of the variables, and the constrained nature of the problem, we have implemented a genetic algorithm [25]. This approach has been widely used to solve the route design and frequency optimization problem in BRT systems [26, 27, 28, 5]. In our case, however, the algorithm is not driven by the evaluation of a given objective function, it is driven instead by the result of the CA based simulations. This so-called simheuristic approach has the advantage of properly taking into account the stochastic nature of the bus movement and interactions [29, 30].

In our genetic algorithm, each specimen in the population corresponds to a distribution of buses among the available bus services and is characterized by a chromosome. A chromosome is a string of binary genes that contains the information of how many buses are assigned to each bus service. To evaluate the mating probability of the specimens in a generation, the so-called roulette-wheel rule has been implemented using the simulated bus flow of each specimen as its fitness. In addition, we have introduced elitism, which means that the best specimen of a generation directly propagates to the next one. The algorithm stops when the historical best specimen does not change after a given number of generations.

Figures 7 and 8 show the results of the optimization as a function of the bus density when three (E1, E3 and E5) and four bus services are in operation, respectively. In all cases, the dwell time has been randomly chosen at each stop using a Poisson distribution with mean $\tau = 15$ s. As shown in the upper panels of the Figure, two different substation assignments have been considered in each case, always making use of the three available docking bays. In Figures 7 and 8, panels (a) and (d) show the distribution of buses that maximizes the bus flow. The error bars shown correspond to the range within which the overall bus flow changes by less than 1%. Panels (b) and (e) depict the bus flow for individual bus services and for the entire system. Panels (c) and (f) show the average

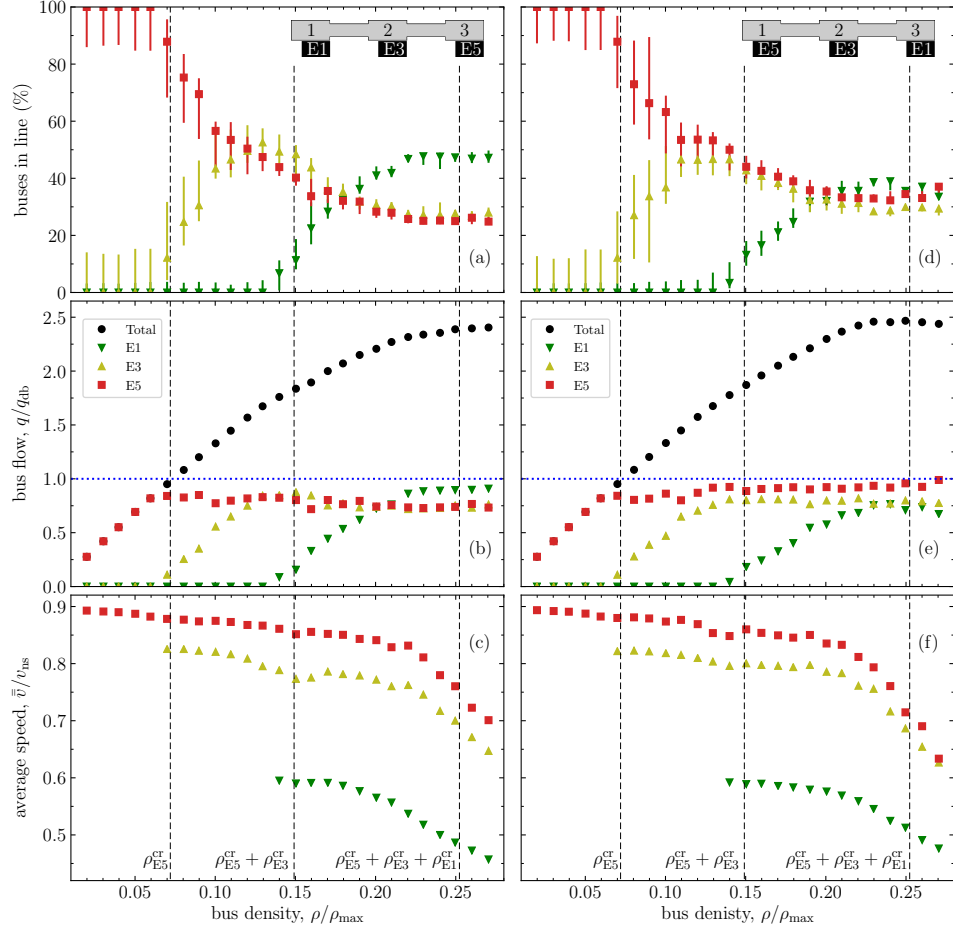


Figure 7: (color online) Results of the flow optimization for different bus densities when the services E1, E3 and E5 are in operation. The diagrams in the upper panels depict the two substation assignments that have been considered. Panels (a), (b) and (c) show the optimal bus distribution, the bus flow, and the average bus speed, respectively, for assignment {E1;E3;E5}. Panels (d), (e) and (f) show the optimal bus distribution, the bus flow, and the average bus speed, respectively, for assignment {E5;E3;E1}. The error bars in panels (a) and (d) represent the range for which changes in the bus flow are smaller than 1%. In panels (b) and (e) the circles represent the overall bus flow in the system, the horizontal dotted line represents the maximum bus flow for a single docking bay. The vertical dashed lines indicate the position of the critical densities as specified.

speed for each bus service.

As a first remark, it is important to note that the algorithm is robust and the optimization results exhibit a coherent evolution as the bus density increases. This is a promising result with regard to the future implementation of an algorithm

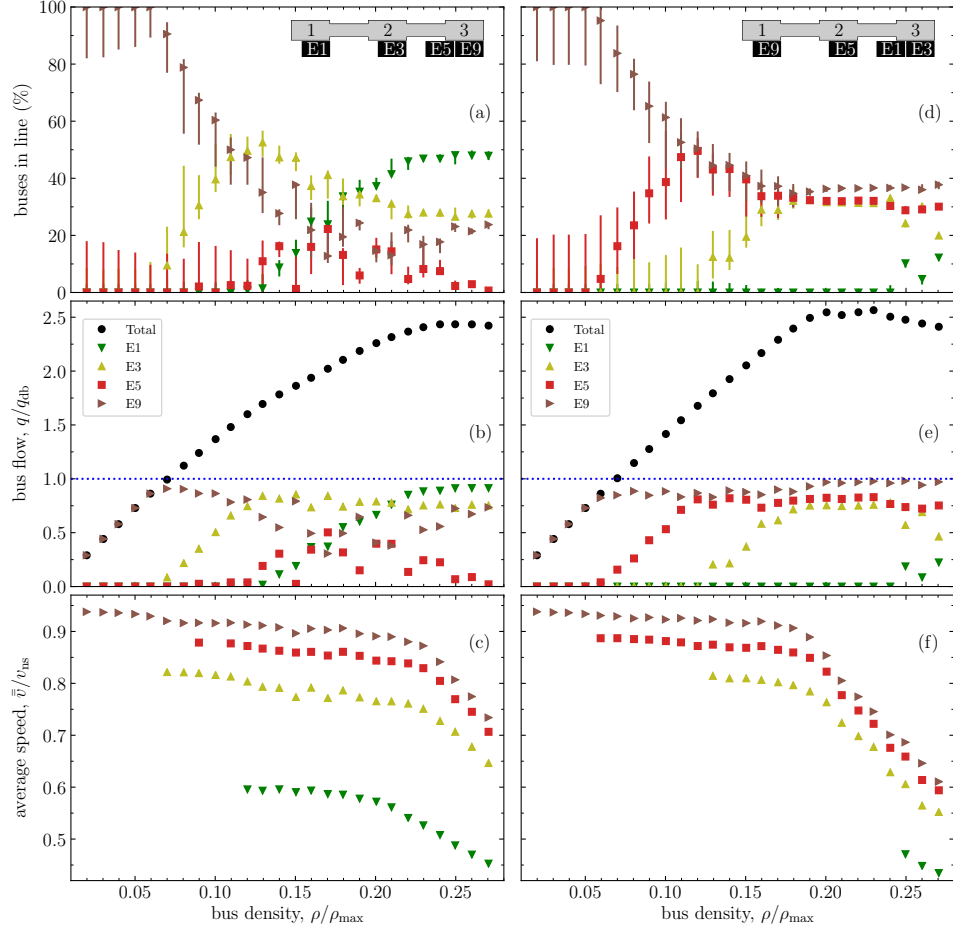


Figure 8: (color online) Results of the flow optimization for different bus densities when the services E1, E3, E5 and E9 are in operation. The diagrams in the upper panels depict the two substation assignments that have been considered. Panels (a), (b) and (c) show the optimal bus distribution, the bus flow, and the average bus speed, respectively, for substation assignment {E1;E3;E5-E9}. Panels (d), (e) and (f) show the optimal bus distribution, the bus flow, and the average bus speed, respectively, for substation assignment {E9;E5;E1-E3}. The error bars in panels (a) and (d) represent the range for which changes in the bus flow are smaller than 1%. In panels (b) and (e) the circles represent the overall bus flow in the system.

based on CA simulations to solve the route design and frequency optimization problem.

At low densities, as expected, the optimization reveals that to maximize the bus flow only the fastest service, E5 in Figure 7 and E9 in Figure 8, must be used. However, as the number of buses increases, so does the bus flow. When

the bus flow for the fastest line is close to the maximum bus flow for a single docking bay, q_{db} , the system avoids the creation of significant queues by assigning buses to the second-fastest service. An exception to this behaviour can be identified in the data shown in Figure 8(a), in this case services E5 and E9 share the same docking bay and in consequence the second service to enter into operation as the bus density increases is E3. As the second fastest service reaches bus flow levels close to q_{db} , a third service enters into operation. We could summarize the results at low densities as follow: in the optimal configuration buses are assigned to the fastest available service as long as significant queues are avoided at the docking bays, as the bus density increases the bus services enter into operation ordered from the fastest to the slowest, the slowest service sharing a docking bay is neglected in the optimal configuration.

In Figure 8(a), there is a significant fluctuation in the optimal results for lines E5 and E9 for densities between $0.12\rho_{max}$ and $0.25\rho_{max}$. These fluctuations evidence the metastability of the solutions when two bus services share the same docking bay. In analogy with Figure 6(a), in this region the efficiency of the system is independent of the bus distribution among these services. A similar metastable regime seems to appear for densities above $0.25\rho_{max}$ for services E1 and E3 in Figure 8(d). In general, we note that outside the metastable regions, the slowest service sharing a substation is neglected. This result could be generalized to conclude that sharing of docking bays by two or more different bus services, even at a single station, tends to harm the system's performance and should be avoided.

In panels (c) and (f) of Figures 7 and 8 there is evidence of the interaction between buses stopping at different docking bays, whenever a new bus service enters into operation, a small but sizeable step-like reduction in the average speed of the bus services already in operation is observed. It is because of these interactions that the maximum observed bus flow in Figures 7 and 8 is significantly lower than the expected $3q_{db}$ (as three docking bays are in operation), they also account for the bus flow saturation at densities well below the accumulated critical density $\rho_{E5}^{cr} + \rho_{E3}^{cr} + \rho_{E1}^{cr}$ in Figure 7.

At large densities, formation of queues is unavoidable and is evidenced by the saturation of the bus flow and the fast reduction of the average bus speed as the number of buses increases, for all bus services. Remarkable differences between the two substation assignments shown in Figures 7 and 8 are evident at high bus densities. The strong dependence of the optimal bus distribution on the substation assignment is a consequence of the interaction between buses at the stations and its observation and study is an evident advantage of our CA based method to study bus dynamics in BRT systems.

A common feature can be identified from panels (b) and (e) in Figures 7 and 8. In the optimal bus distribution at large densities only one bus service exhibits a bus flow close to q_{db} while the other bus service retain bus flow values always be-

low $0.8q_{\text{db}}$. According to the results shown in Figure 5, this observation implies that significant queues only form at the substation where the service with the largest flow stops. Notably, in the optimal configuration, the service with the largest bus flow corresponds in all cases to the bus service assigned to substation 1. This result agrees with our previous observation of the bus flow configuration when two bus services (E1 and E9) are implemented, it could thus be generalized. As discussed in the Supplementary Material, Ref. [24], moving the queues to substation 2 or substation 3, by switching the substation assignment, leads to a bus flow reduction of up to 13% with respect to the optimal configuration. This conclusion can be extrapolated to any working BRT system to state that queues at a given BRT station should always be located at substation 1, this is the first substation the buses encounter on arrival.

Also from panels (b) and (e) in Figures 7 and 8, it can be observed that the maximal bus flow for the bus service assigned at substation 1 depends on its average speed. The faster the bus service, the closer its maximal bus flow is to q_{db} . This effect can be understood in terms of the existing relation between the queue length and the bus flow shown in Figure 5. When service E1 stops at substation 1, relatively small queues are expected at every station in the optimal configuration at high densities. On the other hand, when service E9 stops at substation 1, much longer queues are expected to form every nine stations. However, as suggested by the system's maximal bus flow in Figures 7 and 8, the system performs slightly better in the cases where the fastest bus service is assigned to substation 1. To confirm this observation, we have optimized the bus flow with services E1, E3 and E5, under different substation assignments and at a density $\rho = 0.24\rho_{\text{max}}$. The results are shown in the Supplementary Material, Ref. [24], they reveal that bus flow improvements as large as 5.6% can be obtained if the fastest service stops at substation 1 and the slowest service stops at substation 3. This is a result that could as well be applied to any BRT system in the world to improve the bus flow and thus the passenger transport capacity. However, the length of the queues needs to be considered, as suggested by the reduction in the overall bus flow at densities above $0.24\rho_{\text{max}}$ for assignment {E9;E5;E1-E3} in Figure 8(e). This downturn is an indication that the queues at substation 1 at the stations where service E9 stops become long enough as to interfere with the bus movement at adjacent stations.

5. Summary

We have studied the bus flow in a Bus Rapid Transit (BRT) system by means of a combination of a cellular automata (CA) model and a genetic algorithm. The CA model is an adaptation of the Nagel-Schreckenberg (NaSch) model where additional rules have been introduced to properly reproduce bus movements and interactions, including the behaviour near the stations.

The CA model was initially validated by studying of the bus flow with only one bus service in operation, with either an uniform or randomly chosen dwell

time. When the dwell time is uniform, the fundamental diagram for each bus service can be divided into the uncongested and congested regimes. By determination of the effective dwell time in these two regimes, the critical bus density (which marks the crossover from the uncongested to the congested regime) can be readily calculated. If the dwell time is randomly chosen, which corresponds to a more realistic case, queues appear at any density and the model successfully reproduces the theoretical dependence of the queues' length on the bus flow, which is independent of the bus service. The capability of the CA model to account for the interaction between buses and the bus queueing is identified as a key advantage of our approach.

As more bus services are implemented, the bus flow depends not only on the bus density but also on the bus distribution among the available bus services and on how the bus services are assigned to the available docking bays at the stations. The latter dependence is a consequence of the interaction between buses and cannot be predicted by the standard objective function methods where the interaction between buses is neglected. These interaction are intrinsic in our model, and it allows the study of their impact on the overall bus flow.

We demonstrate that given a set of bus services there is always an optimal bus distribution among the bus services in operation for which the bus flow in the system is maximized. Moreover, the optimal bus distribution strongly depends on how the substations are assigned to the different bus services at the stations. We have implemented a genetic algorithm that evolves with the results of the simulations to study the evolution of this optimal bus distribution with the bus density. From our results we are able to extract the following guidelines, which could enhance the performance of BRT systems around the globe:

- In case queues appear, they should appear at substation 1, this is the first one that the buses encounter on arrival.
- The fastest bus service should be assigned to substation 1 and the slowest bus service should be assigned to substation 3.
- Docking bay sharing by two or more bus services is, in general, harmful to the performance of the system and should be avoided. The bus flow optimization shows that when two services share the same docking bay, the slowest one tends to be suppressed in the optimal configuration.
- Due to the interaction between buses at large bus densities, the capability of a BRT system is smaller than the capability of a single docking bay multiplied by the number of available docking bays at the stations.

The genetic algorithm has proven to be statistically robust and the results of the optimization exhibit coherence as the bus density increases. This is a promising result with regard to the future implementation of a CA based genetic algorithm to solve the route design and frequency optimization problem in BRT systems.

Acknowledgement

We would like to thank Prof. Martha Cobo and Prof. Manuel Figueredo at the Faculty of Engineering of Universidad de La Sabana for the hardware support provided to perform the simulations appearing in this paper.

This research did not receive any specific grant from funding agencies in the public, commercial, or not-for-profit sectors.

References

- [1] L. Wright, W. Hook, The BRT Planning Guide, 4th Edition, Institute for Transportation & Development Policy, New York, 2017 (2017).
URL <https://www.itdp.org/2017/11/16/the-brt-planning-guide/>
- [2] H. Levinson, S. Zimmerman, J. Clinger, G. Rutherford, Bus Rapid Transit: An Overview, *Journal of Public Transportation* 5 (2) (2002) 1–30 (Jun. 2002). doi:10.5038/2375-0901.5.2.1.
URL <http://scholarcommons.usf.edu/jpt/vol5/iss2/1/>
- [3] Global BRTData.
URL <https://brtdata.org/>
- [4] J. L. Walteros, A. L. Medaglia, G. Riao, Hybrid Algorithm for Route Design on Bus Rapid Transit Systems, *Transportation Science* 49 (1) (2015) 66–84 (Feb. 2015). doi:10.1287/trsc.2013.0478.
URL <http://pubsonline.informs.org/doi/abs/10.1287/trsc.2013.0478>
- [5] Y. Yi, K. Choi, Ajou University, Y.-J. Lee, Optimal Limited-stop Bus Routes Selection Using a Genetic Algorithm and Smart Card Data, *Journal of Public Transportation* 19 (4) (2016) 178–198 (Dec. 2016). doi:10.5038/2375-0901.19.4.11.
URL <http://scholarcommons.usf.edu/jpt/vol19/iss4/11/>
- [6] S. Zhong, L. Zhou, S. Ma, N. Jia, L. Zhang, B. Yao, The optimization of bus rapid transit route based on an improved particle swarm optimization, *Transportation Letters* (2016) 1–12 (Dec. 2016). doi:10.1080/19427867.2016.1258972.
URL <https://www.tandfonline.com/doi/full/10.1080/19427867.2016.1258972>
- [7] G. Soto, H. Larrain, J. C. Muoz, A new solution framework for the limited-stop bus service design problem, *Transportation Research Part B: Methodological* 105 (2017) 67–85 (Nov. 2017). doi:10.1016/j.trb.2017.08.026.
URL <https://linkinghub.elsevier.com/retrieve/pii/S0191261517303132>

- [8] F. Martnez, M. G. Baldoqun, A. Mauttone, AND SOLUTION METHOD TO A SIMULTANEOUS ROUTE DESIGN AND FREQUENCY SETTING PROBLEM FOR A BUS RAPID TRANSIT SYSTEM IN COLOMBIA, *Pesquisa Operacional* 37 (2) (2017) 403–434 (Aug. 2017). doi:10.1590/0101-7438.2017.037.02.0403.
URL http://www.scielo.br/scielo.php?script=sci_arttext&pid=S0101-74382017000200403&lng=en&tlng=en
- [9] E. Ruano-Daza, C. Cobos, J. Torres-Jimenez, M. Mendoza, A. Paz, A multiobjective bilevel approach based on global-best harmony search for defining optimal routes and frequencies for bus rapid transit systems, *Applied Soft Computing* 67 (2018) 567–583 (Jun. 2018). doi:10.1016/j.asoc.2018.03.026.
URL <https://linkinghub.elsevier.com/retrieve/pii/S1568494618301480>
- [10] A. Cain, G. Darido, M. R. Baltes, P. Rodriguez, J. C. Barrios, Applicability of Bogota’s Transmilenio BRT system to the United States, Tech. rep., National Bus Rapid Transit Institute (NBRTI), Center for Urban Transportation Research (CUTR), University of South Florida (2006).
- [11] F. J. Pea, A. J. Martn, A. Mateos, Optimising TransMilenio BRT system operation: a mathematical model, *International Journal of Operational Research* 25 (4) (2016) 416 (2016). doi:10.1504/IJOR.2016.075289.
URL <http://www.inderscience.com/link.php?id=75289>
- [12] A. Tirachini, D. A. Hensher, Bus congestion, optimal infrastructure investment and the choice of a fare collection system in dedicated bus corridors, *Transportation Research Part B: Methodological* 45 (5) (2011) 828–844 (Jun. 2011). doi:10.1016/j.trb.2011.02.006.
URL <http://linkinghub.elsevier.com/retrieve/pii/S0191261511000208>
- [13] K. Nagel, M. Schreckenberg, A cellular automaton model for freeway traffic, *Journal de Physique I* 2 (12) (1992) 2221–2229 (Dec. 1992). doi:10.1051/jp1:1992277.
URL <http://www.edpsciences.org/10.1051/jp1:1992277>
- [14] S. Maerivoet, B. De Moor, Cellular automata models of road traffic, *Physics Reports* 419 (1) (2005) 1–64 (Nov. 2005). doi:10.1016/j.physrep.2005.08.005.
URL <http://linkinghub.elsevier.com/retrieve/pii/S0370157305003315>
- [15] K. Nagel, D. E. Wolf, P. Wagner, P. Simon, Two-lane traffic rules for cellular automata: A systematic approach, *Physical Review E* 58 (2) (1998) 1425–1437 (Aug. 1998). doi:10.1103/PhysRevE.58.1425.
URL <https://link.aps.org/doi/10.1103/PhysRevE.58.1425>

- [16] T. Chmura, B. Herz, F. Knorr, T. Pitz, M. Schreckenberg, A simple stochastic cellular automaton for synchronized traffic flow, *Physica A: Statistical Mechanics and its Applications* 405 (2014) 332–337 (Jul. 2014). doi:10.1016/j.physa.2014.03.044.
URL <https://linkinghub.elsevier.com/retrieve/pii/S0378437114002398>
- [17] Y.-S. Qian, X. Feng, J.-W. Zeng, A cellular automata traffic flow model for three-phase theory, *Physica A: Statistical Mechanics and its Applications* 479 (2017) 509–526 (Aug. 2017). doi:10.1016/j.physa.2017.02.057.
URL <http://linkinghub.elsevier.com/retrieve/pii/S0378437117301693>
- [18] X. Ruan, J. Zhou, H. Tu, Z. Jin, X. Shi, An improved cellular automaton with axis information for microscopic traffic simulation, *Transportation Research Part C: Emerging Technologies* 78 (2017) 63–77 (May 2017). doi:10.1016/j.trc.2017.02.023.
URL <http://linkinghub.elsevier.com/retrieve/pii/S0968090X17300645>
- [19] H. Yamamoto, D. Yanagisawa, K. Nishinari, Velocity control for improving flow through a bottleneck, *Journal of Statistical Mechanics: Theory and Experiment* 2017 (4) (2017) 043204 (Apr. 2017). doi:10.1088/1742-5468/aa5a73.
URL <http://stacks.iop.org/1742-5468/2017/i=4/a=043204?key=crossref.9f7c413f52f27facef42fd2be469aae2>
- [20] S. A. Rojas-Galeano, C. A. R. Garzn, A discrete Model of TransMilenio Station Occupation: Representation and algorithms, *Revista de Ingeniera* 40 (2014) 6 (2014).
- [21] A. Tomoeda, K. Nishinari, D. Chowdhury, A. Schadschneider, An information-based traffic control in a public conveyance system: Reduced clustering and enhanced efficiency, *Physica A: Statistical Mechanics and its Applications* 384 (2) (2007) 600–612 (Oct. 2007). doi:10.1016/j.physa.2007.05.047.
URL <https://linkinghub.elsevier.com/retrieve/pii/S0378437107006012>
- [22] R. Widanapathirana, J. M. Bunker, A. Bhaskar, Modelling the BRT station capacity and queuing for all stopping busway operation, *Public Transport* 7 (1) (2015) 21–38 (Mar. 2015). doi:10.1007/s12469-014-0095-y.
URL <http://link.springer.com/10.1007/s12469-014-0095-y>
- [23] M. Schreckenberg, A. Schadschneider, K. Nagel, N. Ito, Discrete stochastic models for traffic flow, *Physical Review E* 51 (4) (1995) 2939–2949 (Apr. 1995). doi:10.1103/PhysRevE.51.2939.
URL <https://link.aps.org/doi/10.1103/PhysRevE.51.2939>

- [24] M. A. Uribe-Laverde, W. Oquendo, Supplementary Material (2019).
- [25] K. Deb, An introduction to genetic algorithms, *Sadhana* 24 (4-5) (1999) 293–315 (Aug. 1999). doi:10.1007/BF02823145.
URL <http://link.springer.com/10.1007/BF02823145>
- [26] C. Sun, W. Zhou, Y. Wang, Scheduling Combination and Headway Optimization of Bus Rapid Transit, *Journal of Transportation Systems Engineering and Information Technology* 8 (5) (2008) 61–67 (Oct. 2008). doi:10.1016/S1570-6672(08)60039-2.
URL <http://linkinghub.elsevier.com/retrieve/pii/S1570667208600392>
- [27] Y. Y. Ulusoy, S. I.-J. Chien, Optimal bus service patterns and frequencies considering transfer demand elasticity with genetic algorithm, *Transportation Planning and Technology* 38 (4) (2015) 409–424 (May 2015). doi:10.1080/03081060.2015.1026101.
URL <http://www.tandfonline.com/doi/full/10.1080/03081060.2015.1026101>
- [28] H.-z. Qu, S. I. J. Chien, X.-b. Liu, P.-t. Zhang, A. Bladikas, Optimizing bus services with variable directional and temporal demand using genetic algorithm, *Journal of Central South University* 23 (7) (2016) 1786–1798 (Jul. 2016). doi:10.1007/s11771-016-3232-8.
URL <http://link.springer.com/10.1007/s11771-016-3232-8>
- [29] A. A. Juan, J. Faulin, S. E. Grasman, M. Rabe, G. Figueira, A review of simheuristics: Extending metaheuristics to deal with stochastic combinatorial optimization problems, *Operations Research Perspectives* 2 (2015) 62–72 (Dec. 2015). doi:10.1016/j.orp.2015.03.001.
URL <http://linkinghub.elsevier.com/retrieve/pii/S221471601500007X>
- [30] M. Chica, A. A. Juan Prez, O. Cordon, D. Kelton, Why Simheuristics? Benefits, Limitations, and Best Practices When Combining Metaheuristics with Simulation, *SSRN Electronic Journal* (2017). doi:10.2139/ssrn.2919208.
URL <http://www.ssrn.com/abstract=2919208>